Precise Synthesis of ABA Triblock Copolymers Comprised of Poly(ethylene oxide) and Poly(β-benzyl-L-aspartate): A Hierarchical Structure Inducing Excellent Elasticity

Shinji Tanaka,[†,‡] Atsuhiko Ogura,[‡] Tatsuo Kaneko,[†] Yoshishige Murata,[‡] and Mitsuru Akashi*[,†,§]

Department of Nanostructured and Advanced Materials, Graduate School of Science and Engineering, Kagoshima University, 1-21-40, Korimoto, Kagoshima 890-0065, Japan; Tsukuba Research Laboratory, NOF Corporation, 5-10 Tokodai, Tsukuba, Ibaraki 300-2635, Japan; and Department of Molecular Chemistry, Graduate School of Engineering, Osaka University, 2-1, Yamadaoka, Suita, Japan

Received September 29, 2003; Revised Manuscript Received December 10, 2003

ABSTRACT: ABA triblock copolymers comprised of poly(β-benzyl-L-aspartate) (PBLA) as an A segment and poly(ethylene oxide) (PEO) as the B segment were precisely synthesized by a ring-opening polymerization of the *N*-carboxyanhydride of BLA initiated from amines at both terminals of the PEO chain. The copolymers have a number-average molecular weight (M_n) of 1.5×10^4−3.6×10^4 and a monodisperse molecular weight distribution in the range 1.04−1.07. The copolymer films casted from a dichloromethane solution were flexible and elastic despite their low M_n. The film formed a hierarchical structure, i.e., the chains adopted an α-helix−7_2 helix−α-helix conformation and was highly crystallized, forming a long-range ordering structure which resulted in a rodlike construct arranged like ripples, as confirmed by Fourier transformed infrared spectroscopy, X-ray diffraction, and atomic force microscopy. Differential scanning calorimetry confirmed that the film showed a melting endotherm of the PEO segment at 313−326 K depending on the PBLA content. The film became very soft and behaved like rubber above the melting temperature. When the film was successively cooled, the crystalline diffraction became less intense, especially in terms of the PBLA segments whose conformation partially transformed from α-helices to β-sheets, and the film showed enhanced strength and drastically increased deformation, with a strain of more than 500% accompanied by a necking phenomenon. The relationship between the mechanical properties and the structure is also discussed.

Introduction

To combine mechanical strength and flexibility, as well as biocompatibility and biostability, is very important for the molecular design of novel biomedical macromolecules. Poly(L-amino acid)s present outstanding physicochemical and biological properties, including mechanical properties, nontoxicity, and lower antigenicity,[1] which has allowed the use of poly(L-amino acid)s in many biomedical and clinical applications, such as for hemodialyzers, wound dressings, and artificial skin substitutes.[2−5]

Poly(γ-benzyl-L-glutamate) (PBLG) and poly(β-benzyl-L-aspartate) (PBLA) are widely investigated as typical biopolymers which form specific secondary structures, such as an α-helix, β-sheet, or coil, and show structural transitions upon environmental changes that alter the arrangement of the hydrogen bonding. Since PBLG and PBLA are hydrophobic, they can be handled as solid materials in water. However, they are so brittle that it is difficult to apply them to living organs without combing them with other techniques.

Poly(ethylene oxide) (PEO) is an amphiphilic macromolecule that has been studied in a wide range of chemical, biomedical, and industrial applications because PEO has useful properties such as high solubility, excellent processability, strong interactions with metal ions, ease of chemical modification, and biological compatibility.[6−10] Although PEO has a molecular weight of 20 000 or less and is not biodegradable, it is quite safe because it can be absorbed in a living body and excreted through the kidneys.[8,11]

To develop materials with the characteristics of both polypeptides and PEO, various copolymers comprised of both segments have been investigated. Diblock copolymers comprised of PBLA and PEO can self-organize to form stable micelles at a very low critical micelle concentration with a monodisperse diameter below 0.1 μm and have been used as a passive drug delivery system for antitumor agents.[12,13] ABA symmetrical triblock copolymers comprised of a hydrophobic polypeptide as A segment and a hydrophilic polyether as B segment were also investigated. They usually undergo a phase separation in the solid state inducing biocompatability and antithrombogenicity. Kugo et al. synthesized and characterized ABA triblock copolymers comprised of PBLG or PBLA and PEO.[14] These copolymers had good permeability for water or gas and were considered to be useful as a substrate for cell culture, implants, or wound dressing materials. Cho et al. reported the microphase separation of a copolymer comprised of PBLG and PEO and the adhesion behavior of fibroblasts and platelets onto Langmuir−Blodgett or cast films.[15,16] Floudas et al. discovered that the secondary structure of PBLG was controlled by the incorporation of PEO in the middle block.[17] Despite these vigorous studies, very few attempts have been made to investigate the mechanical properties of these copolymers in bulk. In particular, no study has been performed on

† Kagoshima University.
‡ NOF Corporation.
§ Osaka University.
* Corresponding author: Tel +81-99-282-8320; Fax +81-99-255-1229; e-mail akashi@chem.eng.osaka-u.ac.jp.

10.1021/ma035472n CCC: $27.50
Published on Web 01/24/2004

copolymers with a high content of PEO whose M_n was over 10 000.

In the present study, we examined the organizational behavior in terms of crystallinity relating to the thermal and mechanical properties of cast films of ABA triblock copolymers comprised of PBLA as the A segment and PEO with molecular weights of 11 000 and 20 000 as the B segment. The thermal treatment of these film induced an α-helix to β-sheet transformation in the PBLA segments, enhancing the maximal strength and drastically increasing the elongation with necking.

Experimental Section

Materials. PEO with amino groups at both ends is commercially available (M_n = 11 000 and 20 000, NOF Corporation, Japan) and was used as received as the initiator of the polymerization of β-benzyl-L-aspartate *N*-carboxyanhydride (BLA−NCA)). Dehydrated dichloromethane (Kanto Kagaku, Japan) and *N*,*N*-dimethylformamide (DMF, water content <30 ppm, Wako Chemical Co. Ltd., Japan) were used for the polymerization as received. BLA−NCA was prepared by the method of Goodman et al.[18]

Copolymerization Procedures. The copolymers were precisely synthesized in the following procedure. The ring-opening polymerization of BLA−NCA was performed without any catalyst for 24 h at 313 K under a nitrogen atmosphere, initiating from an amine-terminated PEO (10% w/v) in a mixture of dichloromethane/DMF (9/1, v/v), while varying the BLA−NCA composition in the feed from 5 to 10%. The polymerization proceeded homogeneously, and the reaction solution was poured into a large amount of hexane/ethyl acetate (1/1, v/v) to precipitate the white solid. The products were washed with hexane and then dried in vacuo at room temperature, yielding the p(BLA−EO−BLA) triblock copolymers (yield: over 98 wt % on the basis of PEO recovery). The structures were confirmed by infrared (IR) spectroscopy and proton nuclear magnetic resonance (^{1}H NMR).

Polymer Characterization. The M_n, weight-average molecular weight (M_w), and polydispersity (M_w/M_n) of the copolymers were measured by gel permeation chromatography (GPC) using a TOSOH SG-8020 liquid chromatograph equipped with a PEO-calibrated TSK gel column (G3,000H HR or G4,-000H HR) and an internal RI detector (RI-8022). DMF containing 10 mM LiCl was used as an eluent at a flow rate of 0.8 mL/min at 313 K.

The ^{1}H NMR spectra of the copolymers were measured at 353 K in a solvent of DMSO-d_6 on a JEOL JNM-EX270 FT NMR spectrometer to estimate the copolymer compositions and the molecular weights of PBLA blocks, using the residual proton resonance of the deuterated solvent as the internal standard (2.55 ppm).

The FT-IR spectra of the copolymer films were measured on a Perkin-Elmer Spectrum One spectropolarimeter between 4000 and 400 cm^{-1}. The films were prepared at room temperature by casting the copolymer solution in dichloromethane (5%, w/v) on a Teflon film.

Crossed-polarizing microscopic images were taken with an Olympus BX51 microscope equipped with a digital camera and a programmable temperature controller (resolution: ±0.1 K). Specimens were prepared by the cast film from dichloromethane (1 wt % solution) onto glass slides.

X-ray diffractions (XRD) were recorded on an X-ray diffractometer (RINT UltraX18) equipped with a scintillation counter using Cu Kα radiation (40 kV, 200 mA; wavelength = 1.5418 Å), which was monochromated by a parabolic multilayer mirror in transmission geometry. The samples were prepared by casting on a Teflon plate from dichloromethane solution at room temperature.

Atomic force microscope (AFM) topographic images were taken in phase mode with an Asylum research atomic force microscope MFP-3D. Specimens were examined in air with a silicon probe, AC240 (Olympus). The test surface was prepared on a mica plate by casting the specimen from dichloromethane solution.

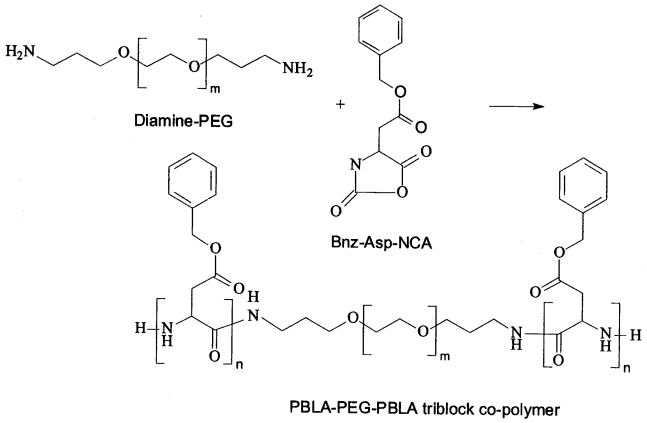

Figure 1. Synthesis of ABA triblock copolymers composed of P(BLA-*block*-EO-*block*-BLA).

The calorimetry experiments were conducted with a Seiko Instrument Inc. DSC-210. All experiments were performed in a nitrogen gas atmosphere heated from 223 to 523 K at a heating rate of 10 K/min. The specimens were cast into the sample pan and were evaporated for 12 h at room temperature.

The stress−strain curve of a strip of film 2 mm wide was measured by a Yamaden creep meter RE3305 at room temperature with a tensile rate of 1.0 cm/min. Young's modulus was determined from the inclination of the curve within a strain of less than 1%.

Results and Discussion

Precise Synthesis and Characterization of Triblock Copolymers. To prepare the PBLA−PEO−PBLA triblock copolymers with varying degrees of polymerization of the BLA and PEO segments, we performed the ring-opening polymerization of BLA−NCA initiating from the amino terminal groups of PEO with an M_n of 11 000 and 20 000 and a monodisperse molecular weight distribution. The PEO/PBLA molar ratio in the feed ranged from 0.4 to 1.0% in order to control the degree of polymeization of the PBLA segments. The polymerization proceeded homogeneously, and the yields were high. The IR spectra showed the following vibration peaks: 3302 cm^{-1} (m, N−H amide), 2880 cm^{-1} (s, C−H), 1736 cm^{-1} (s, C═O), 1657 cm^{-1} (s, amide I), 1552 cm^{-1} (s, amide II), and 1341, 1258, 1096, 960, 947, 841, 752, 698 cm^{-1}. The synthesized copolymers gave a sharp peak with one top in the GPC curve, as shown in Figure 2a. The M_n, M_w, and M_w/M_n of the copolymers are summarized in Table 1, and the polydispersity settled in a narrow range of 1.04−1.07. The ^{1}H NMR spectra (in DMSO-d_6) showed that all of the polymers presented well-defined NMR spectra with similar characteristics. The spectrum of 20K25 is presented for example in Figure 2b; δ = 7.9 ppm (H, s, −N*H*−), 7.3 ppm (5H, s, arom), 5.1 ppm (2H, benzyl−), 4.6 ppm (2H, m, α-CH_2−), 3.5 ppm (s, −CH_2CH_2O−), and 2.8 ppm (2H, m, β-CH_2−), where the strength of the peak at 3.5 ppm depended on the samples. These results confirmed that copolymerization by the ring-opening reaction with PLA−NCA resulted in monodisperse triblock copolymers containing two PBLA blocks attached at both PEO chain terminals.

The ^{1}H NMR spectra of the triblock copolymers were used to determine the PEO/PBLA ratio from the integration ratio of resonance corresponding to PEO blocks

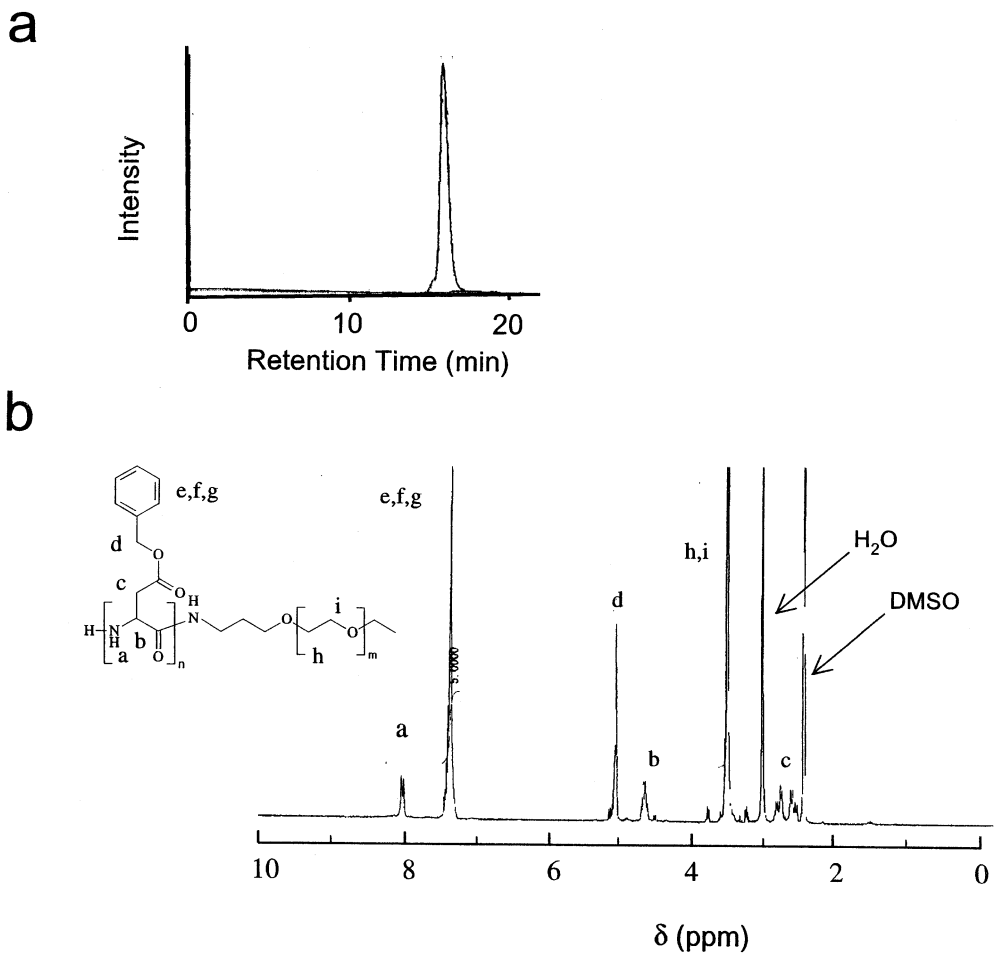

Figure 2. (a) GPC chromatogram and (b) ^{1}H NMR spectrum of the ABA triblock copolymer 20K25. The ^{1}H NMR spectrum was recorded in DMSO-d_6 solution at 353 K.

Table 1. Characterization of the ABA Triblock Copolymers Composed of Poly(BLA-*block*-EO-*block*-PLA)

			triblock copolymers[b]						
desig-nation	M_n of PEO diamine	BLA/EO (mol/mol) in feed	M_n (NMR) $\times 10^{-4}$	M_w (GPC) $\times 10^{-4}$	M_n (GPC) $\times 10^{-4}$	M_w/M_n	DP_n[c] PEO	DP_n[c] PBLA	BLA/EO (mol/mol) in product
11K12	11 000	0.105	1.6	1.6	1.5	1.04	250	12	0.096
11K18	11 000	0.153	1.9	1.7	1.6	1.05	250	18	0.145
11K25	11 000	0.220	2.2	2.4	2.3	1.05	250	25	0.200
20K18	20 000	0.085	2.8	2.9	2.8	1.04	454	18	0.078
20K25	20 000	0.116	3.1	2.8	2.7	1.04	454	25	0.109
20K32	20 000	0.148	3.8	3.8	3.6	1.07	454	32	0.138

[a] BLA refers to β-benzyl-L-aspartate, and EO refers to ethylene oxide. Poly(BLA-*block*-EO-*block*-BLA) was prepared by the ring-opening polymerization of the BLA *N*-carboxyanhydride initiated by the amino terminal groups of diamino-PEO (M_n = 11 000 and 20 000). [b] In 11K*YY* and 20K*YY*, the numbers 11 and 20 refer to the B segment of PEO with an M_n of 11 000 and 20 000, respectively, and *YY* refers to the degree of polymerization of the PBLA A segments estimated by ^{1}H NMR. [c] The number-average molecular weight, M_n, and weight-average molecular weight, M_w, and molecular weight distribution. The M_w/M_n ratio was measured by gel permeation chromatography using PEO standards. [d] The degree of polymerization, DP_n, of the PEO segments was estimated from the M_n of the PEO diamines used as initiators. The DP_n of the PBLA block was determined from the ratio of the integral values of the resonance peaks for PEO segments at 3.6 ppm ($-O-CH_2CH_2-$; 4H) to those for PBLA segments at 7.3 ppm (C_6H_5-; 5H).

at 3.5 ppm ($-CH_2-CH_2-O-$, singlet) and to PBLA blocks at 7.3 ppm (C_6H_5-, singlet). These results are summarized in Table 1. After reprecipitation, all of the resulting triblock copolymers exhibited BLA/EO molar ratios between 90 and 95%, as high as those of the corresponding ratios in the feed solutions (Table 1). This finding strongly suggested that the reaction system was capable of being regulated by the feeding ratio for the same reaction time. The M_n values of the copolymers calculated from the above ^{1}H NMR data corresponded practically with the M_n values measured by the GPC. As described above, ABA triblock copolymers with a monodisperse molecular weight distribution were synthesized by the ring-opening polymerization. They were all soluble in dichloromethane, DMSO, and DMF. The films casted from dichloromethane were translucent and so flexible and tough that they were able to bend without breaking despite the low M_w relative to the polymers being widely applied as a film. The flexibility and toughness could be attributed to specific structures formed by well-defined monodisperse polymers.

Structures. Since the film was translucent, it may have had some domains that scattered the light. We observed the film casted from the dichloromethane

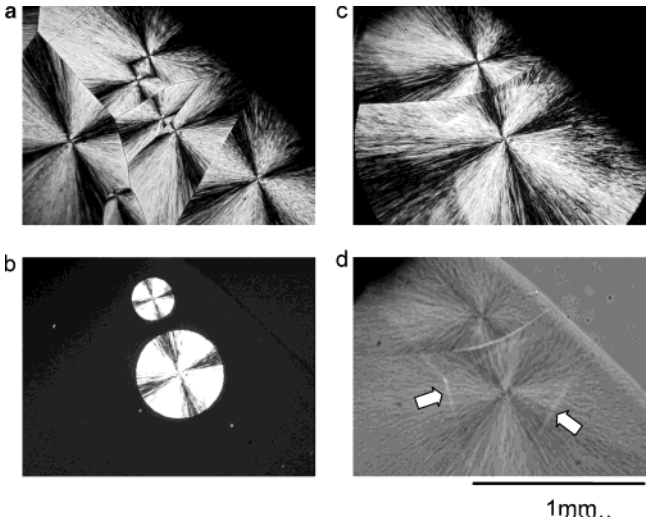

Figure 3. Crossed-polarizing microphotographs of 20K25: (a) the film was as-casted from dichloromethane solution, (b) the film was cooled from the melted state at 333 K to 303 K, (c) the films settled at 303 K for 1 min after the treatment shown in (b), and (d) differential interference micrographs of the same sample as in (c) without the crossed-polarizer. The arrows refer to the interfacial line corresponding to the crystalline interface of the sample (a).

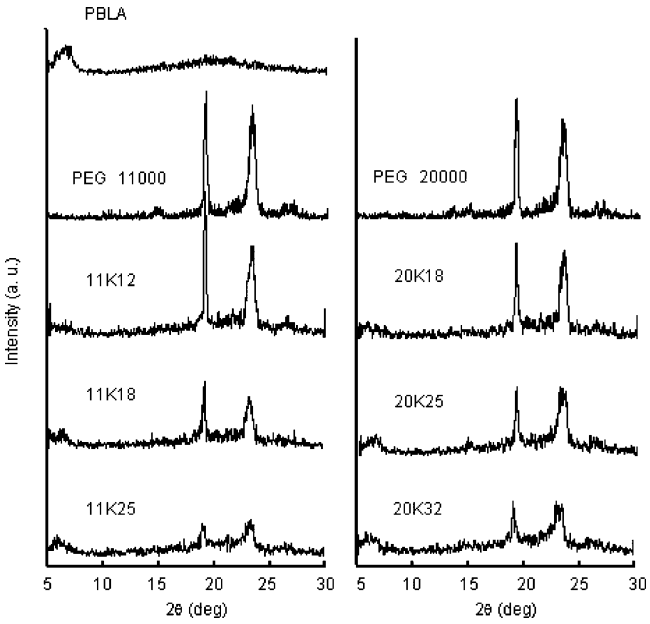

Figure 4. Wide-angle X-ray diffraction patterns of PEOs, PBLA, and the triblock copolymers as-casted from dichloromethane solution.

solution by cross polarizing microscopy. As shown in Figure 3, all of the films were filled with spherulites of various sizes ranging from 10 to 1000 μm, which are also seen in the PEO film. These data suggest that the PEO segments might be well crystallized in all copolymers comprised of high concentrations of PEO (more than 80%). The structure of the copolymers was investigated by WAXD study (Figure 4). The WAXD patterns showed intensive and sharp diffractions at $2\theta = 19°$, 23°, and 26° (θ: diffraction angle) corresponding to 4.7, 3.9, and 3.5 Å, respectively, indicating that the copolymers were well-crystallized. These diffractions were characteristic of PEO crystals where the PEO chains form a 7_2 helix structure with 6 Å per cycle.[19,20] It was clear that the PEO in the middle segment formed a 7_2 helix structure in all of the copolymers. As greater

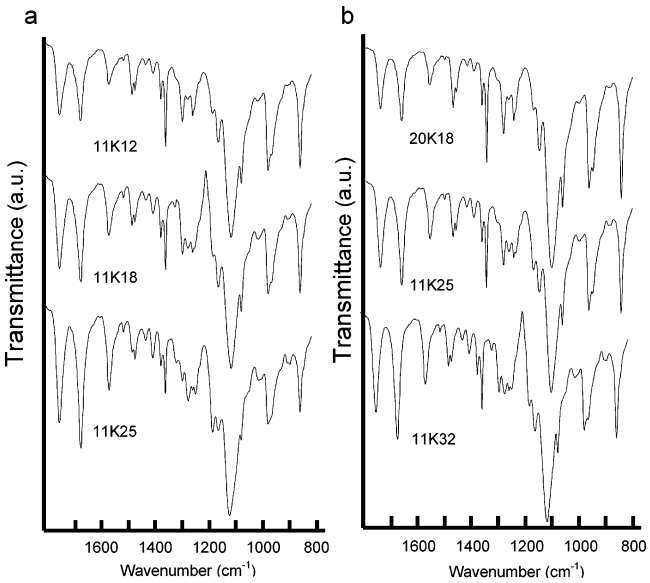

Figure 5. FT-IR spectra of the triblock copolymers as-casted from dichloromethane solution.

lengths of PBLA were combined at both terminals of the PEO, the intensity of these diffraction signals between $2\theta = 16°$ and 30° gradually decreased. Other than the weak diffraction appearing at $2\theta = 5.9°$ corresponding to 15 Å, which appeared in the WAXD diagram of the PBLA homopolymer and was assigned to a nonspecific hexatic arrangement of the α-helical PBLA chains according to the literature,[17] the intensity increased with an increase in the PBLA length. Similar behavior in other polypeptide crystalline segments has been reported in the literature for poly(ϵ-benzyloxycarbonyl-L-lysine)−PEO−poly(ϵ-benzyloxycarbonyl-L-lysine).[21] The appearance of crystalline diffractions from individual homopolymers suggested that the PEO segments segregated from PBLA segments, which affected the PEO organization.

To investigate the secondary structures of the polypeptide blocks in the film in more detail, IR spectroscopy measurements were carried out. Figure 5 shows that the peaks of amide I was at 1650 cm^{-1} and amide II was at 1550 cm^{-1}, thus demonstrating the α-helix conformations which the PBLA homopolymer also adopted.[22] The absorption band at 1630 cm^{-1} characteristic of the β-sheet conformation did not appear in all triblock copolymers.[23,24] In addition, the absorptions were observed at 947 and 847 cm^{-1}, which are characteristic of the crystals of PEO in a 7_2 helix.[9] From these data, these polymers formed a specific secondary structure, an α-helix−7_2 helix−α-helix. Several symmetrical triblock copolymers reported thus far did not exhibit such a conformation because they were too short in their middle PEO segments to form crystals. An α-helix (3.6_1 helix) has a similar pitch as a 7_2 helix (3.5_1 helix), which may be a reason for the mutual influence of these crystals.

Figure 6 shows the SAXD patterns of copolymers with various lengths of PBLA and PEO. In the case of PEO with an M_n of 20 000, broad and weak diffraction peaks were observed at $2\theta = 0.5 \pm 0.2°$ for 20K25 and at $2\theta = 0.6 \pm 0.2°$ for 20K32, corresponding to a long-range periodicity of 290−130 and 220−110 Å, respectively. In the case of PEG with an M_w of 11 000, a diffraction was observed at $2\theta = 0.9 \pm 0.3°$ for 11K25 corresponding to 150−70 Å. These broad SAXD peaks support the forma-

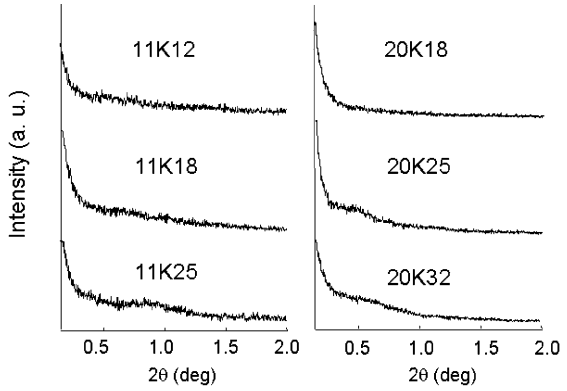

Figure 6. Small-angle X-ray diffraction patterns of the triblock copolymers as-casted from dichloromethane solution.

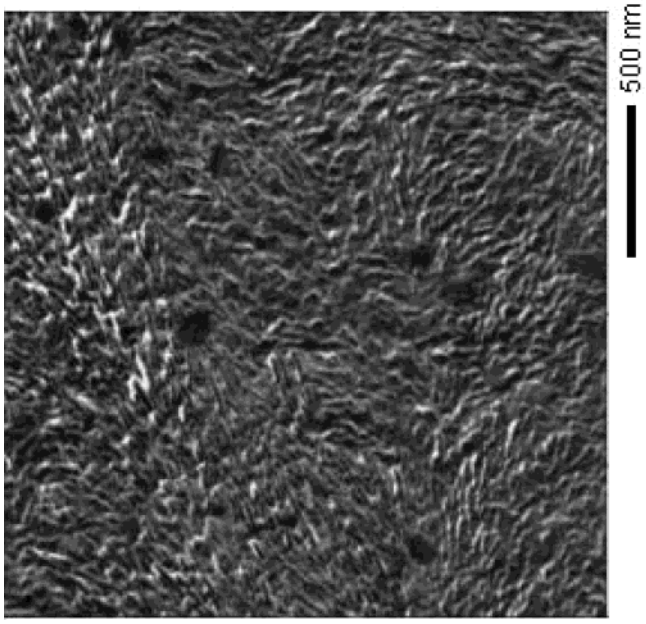

Figure 7. Atomic force microscopic images of the 20K25 film as-casted from dichloromethane solution taken in phase mode.

tion of long-range structures in the copolymer films, although the regularity was low. The long-range period of the copolymer films increased upon decreasing the relative length of the PBLA segments to that of the PEO segments.

The AFM image for the 20K25 cast film in the phase mode is shown in Figure 7. One can see a number of ripplelike constructs arranged with a spacing ranging from 150 to 300 Å, which is almost consistent with the SAXD spacing. The length of a ripple was 700−1000 Å, which approximates the chain length of 20K25, which is estimated at 855 Å on the basis of the calculation that 25 units of PBLA segments forming an α-helix rod were 37.5 Å long, and PEO segments forming a 7_2 helix were 780 Å long. Therefore, the aggregation of the copolymer chains, which may more effectively occur in those copolymers with longer PBLA segments, may be associated with the formation of the ripplelike construct. The AFM images also confirmed that the arrangement of the ripplelike structures created a leaflike large region several hundred nanometers across in scale. Furthermore, as confirmed by optical microscopy, the spherulites were formed over the surface of the film. Thus, the film formed a hierarchical structure which could possibly contribute to the film stiffness, since the crystallized ripple domains formed the framework structure.

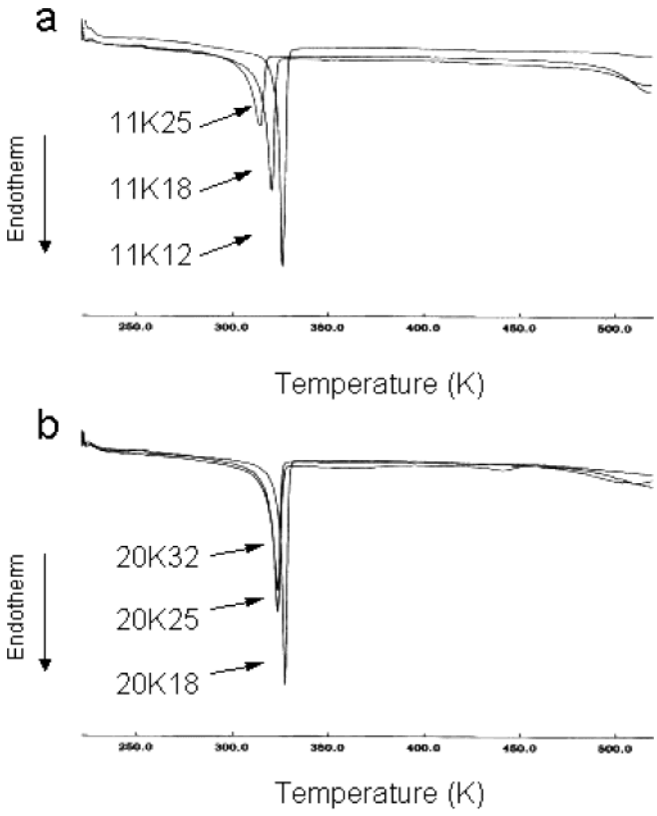

Figure 8. Differential scanning calorimetric thermograms of the triblock copolymers as-casted from dichloromethane solution.

Table 2. Melting Parameters and Young's Modulus, *E*, of the Copolymers

designation	T_m[a] (K)	ΔH[a] (J/mol)	ΔS[a] (kJ/(mol K))	E[b] (MPa)
11K12	325	1.55	4.79	19
11K18	319	1.07	3.36	21
11K25	313	0.80	2.55	18
20K18	326	2.36	7.23	25
20K25	322	1.98	6.13	27
20K32	322	1.83	5.67	22
PEG 11 000	333	2.10	6.31	ND[c]
PEG 20 000	334	3.76	11.27	ND[c]

[a] T_m, ΔH, and ΔS refer to melting temperature, enthalpy change, and entropy change, respectively, measured by differential scanning calorimetry on first heating. ΔH and ΔS were estimated in terms of the molar amount of EO units. [b] E refers to Young's modulus measured from the tensile strength test. [c] ND = not determined.

If the region between the ripples was assumed to be amorphous, then the framework may have sufficient mobility to give the film-enhanced flexibility.

Thermotropic Properties. We investigated the thermal properties of these films. Figure 8 shows DSC thermograms of the copolymers exibiting a sharp endotherm between 313 and 326 K. Since these temperatures are comparable with the melting of PEO crystals (333 K), but were much lower than that of PBLA crystals (above 523 K), the endotherms of these copolymers may be assigned to the melting of the PEO segments. These melting temperatures are summarized in Table 2, and the melting parameters are plotted against the PBLA molar composition in Figure 9. The T_m's of PEO decreased linearly with an increase in the PBLA composition and were independent of the PEO length, as shown in Figure 9a. These results indicated that the crystallinity of PEO was strongly restricted by

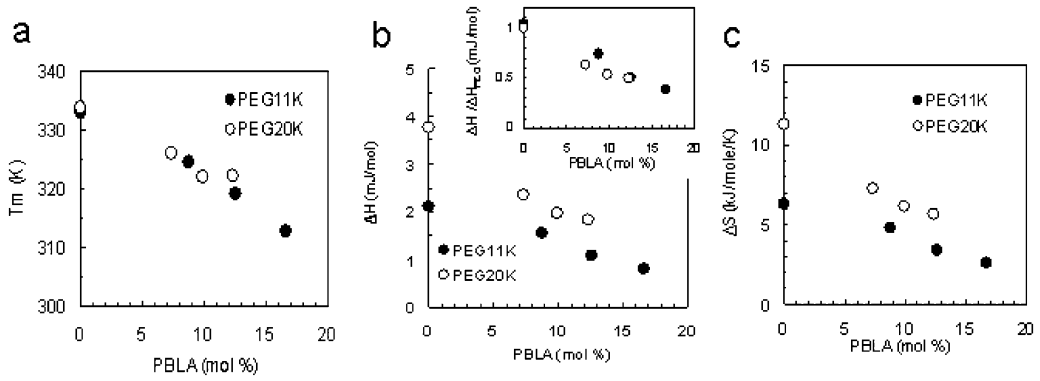

Figure 9. Melting parameters of PEO and the triblock copolymers as-casted from dichloromethane solution obtained from the thermogram of Figure 8. The data were plotted against the PBLA content. (a) Melting temperature, T_m. (b) Melting enthalpy, ΔH. Inset: the ratio of the ΔH value for the triblock copolymer to homopolymer PEO. (c) Melting entropy, ΔS.

the PBLA segments, which may help maintain the solid state. As indicated in the WAXD studies, PEO crystals may become disordered by the influence of the interface with the PBLA crystals.

Figure 9b,c showed the changes in the melting enthalpy and entropy as a function of the PBLA content (data summarized in Table 2). The enthalpies and entropies decreased with an increase in the PBLA content in both PEO systems. We showed the ratio of the ΔH value for the triblock copolymer to ΔH of homopolymer in the inset of Figure 9b. From the results, one can guess that the crystallinity of PEO blocks was reduced by the influence of PBLA blocks although it was difficult to obtain the degree of crystallization of PEO blocks directly from the WAXD diagram due to the overlapping of the amorphous halo for the PBLA blocks with those for the PEO blocks. These results also showed that the crystalline ordering of the PEO chains. The fact that such a small amount of PBLA so strongly affected the crystallinity of the PEO segment may be due to the similarity of the helical conformations between both segments. The interdependence of both blocks may occur at the interfacial region.

We investigated the growing behavior of the spherulites in the 20K25 film by cooling from 333 K, which is higher than the endothermic temperature. Heating to 333 K made the film transparent, but the film did not melt down to a soft, rubbery state. This observation strongly suggested that the PBLA crystal domains, which were small enough not to scatter the visible light, still remained at 333 K and sustained the shape of the film as a framework. Crossed-polarizing microscopic observation suggested that the spherulites disappeared upon heating to 333 K and recrystallized by standing for 5 min following successive cooling cycles at 303 K as shown in Figure 3b. The regenerated spherulites grew larger than the original ones, but the interfacial lines of the original spherulites could still be observed over the regenerated ones, as shown in Figure 3c. Differential interference microscopy in Figure 3d shows more clearly these original interfacial lines, and the newly generated crystals grew beyond the original interfaces. We hypothesize from these observations that the location of the molecules was restricted in the PEG melted state but had sufficient mobility to reconstruct the spherulites freely. In Figure 10a, the WAXD patterns of the original film showed intense crystalline peaks from both PEO and PBLA segments. The intensity of these peaks reduced after the thermal treatment, indicating that the degree of crystalline had decreased.

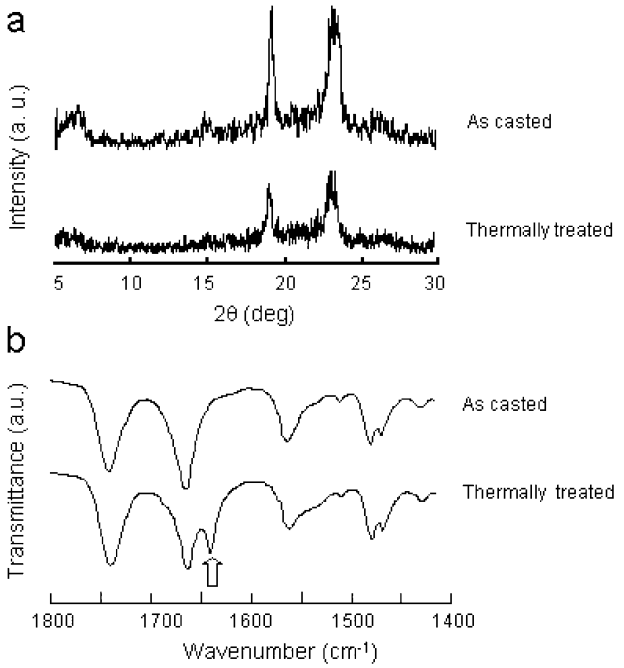

Figure 10. Effects of thermal treatment on the triblock copolymer of the 20K25 film casted from dichloromethane solution on (a) wide-angle X-ray diffraction patterns and (b) FT-IR spectra. Upper: the as-casted film. Lower: the film cooled from 333 to 303 K.

These results were supported by the measurement of the DSC second heating where the T_m, the changes of enthalpies and entropies, decreased (data not shown). Figure 10b shows the FT-IR spectrum of as-casted and thermally treated films. The IR vibration appeared at 1630 cm^{-1} (white arrow) overlapping with the amide I peaks at 1655 cm^{-1} upon thermal treatment, indicating that the PBLA segments partially transformed from α-helices to β-sheets in conformation. The IR peak at 1630 cm^{-1} kept its strength over 24 h, suggesting that the transition from α-helix to β-sheet was irreversible. This conformational change did not occur in the PBLA homopolymer, even after keeping it at the higher temperature of 353 K for a longer time. The amount of absorption at 1630 cm^{-1} increased with an increase in heating time in the case of over 333 K, but the same absorption was not observed for heating below 323 K. A similar thermal−irreversible transition from α-helix to β-sheet has been reported in the case of Alzheimer's β-amyloid protein.[25] The α-helix formed by intrachain hydrogen bonds was broken by the high chain mobility

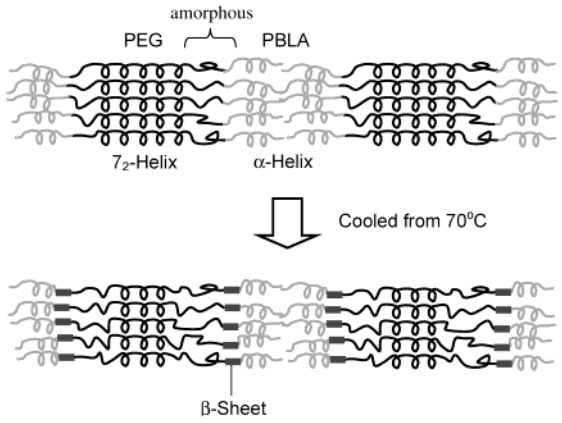

Figure 11. Schematic illustration of the structural change of the triblock copolymers following the heat treatment as shown in Figure 3c.

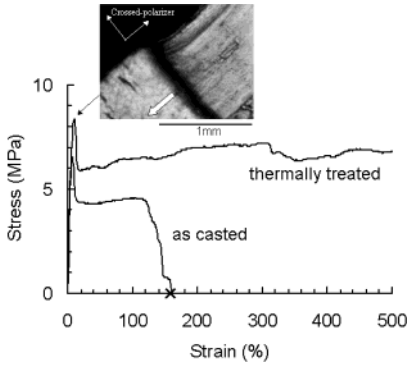

Figure 12. Stress−strain curves of the copolymer of the 20K25 film as-casted from dichloromethane solution and cooled from 333 K. The mark X refers to the breaking point. The inset picture is a crossed-polarizing microscopic image of the film stretched up to strain = 100%, where the film was stretched in a direction (arrow) that formed an angle of 45° to both polarizers. The arrow also shows the transfer of the necking portion by further stretching.

caused by the melted adjacent chains of PEO, and instead a β-sheet was formed by interchain multiple hydrogen bonds. If the PBLA segments in the interfacial region of the PEO domains obtained their chain mobility from the melting PEO segments, then such a conformational change could occur at lower temperatures. This chain arrangement altered by thermal treatment is schematically illustrated in Figure 11 where the amorphous region of PEO blocks can be assumed at the interfacial region based on the general phenomenon that the crystallization of a molecule was interfered with other molecules.

Mechanical Properties. The effects of the thermal treatment on the mechanical properties were investigated by the tensile test. Stress−strain curves of the 20K25 film casted at room temperature from dichloromethane solution are shown in Figure 12. Elastic deformation behavior was obtained by stretching it up to 10% elongation, when the film showed "necking", like the polyethylene film, depicted in the inset of Figure 12. As for the other triblock copolymers, the copolymers with PEO 11 000 showed less elastic deformation, while those copolymers with PEO 20 000 showed elasticity that depended on the PBLA chain length. Young's modulus and the maximal stress of other copolymers are summarized in Table 2 and Figure 13, respectively. Young's modulus was almost constant regardless of the length of the PBLA segments, but the copolymer comprised of PEO with the higher M_n had a higher Young's modulus. The maximal strength of the films showed a lower dependence on the PBLA content and a higher dependence on PEO. The high crystallinity usually gives the film an enhanced Young's modulus. In the present case, the WAXD study showed that the crystallinity of PBLA and PEO showed an opposite dependence on the decrease in PEO composition, which may be one possible reason for the low dependence. Rather than PBLA, the length of the better organized PEO segments more strongly affected the mechanical properties. In 20K25, the fracture took place within 200% elongation, at the point indicated by the cross joint in the curve of Figure 12. In contrast with the as-cast film, the maximal strength upon stretching and elongation after necking were remarkably increased by a thermal treatment at 333 K for 3 h, although little change was shown in Young's modulus as shown. More interestingly, the fracture was not observed within 500% deformation. Crossed-polarizing microscopic imaging (inset in Figure 12) showed that many pieces of the spherulites disappeared following necking to create the striped texture. The necked portion transferred to the white-arrowed area upon further stretching, thus decreasing the region of the spherulites and increasing the region of the striped texture. The crystalline structure of PEO remained in the stripped portion, as confirmed by the X-ray diffraction patterns (data not shown). The difference in the stretching behavior of these films generated by the thermal treatment may be due to the structural change from an α-helix into a β-sheet and the decrease in crystallinity. Since the β-sheet gives the strong interchain interactions, a physical cross-linkage was generated to increase the mechanical strength. The

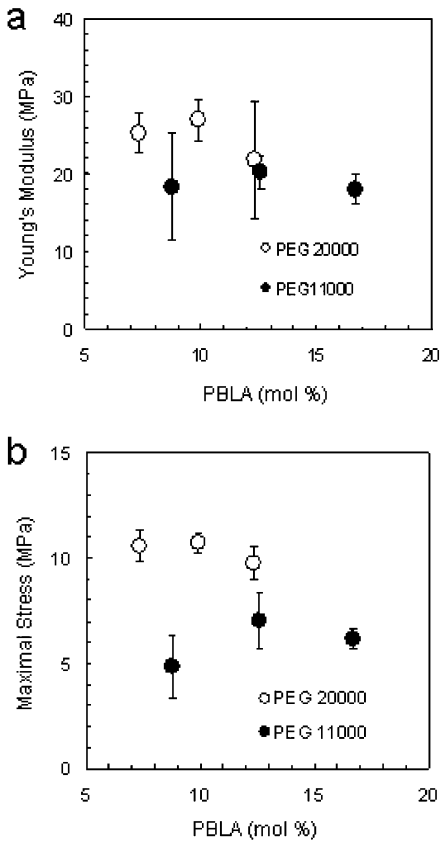

Figure 13. Changes in (a) Young's modulus and (b) maximal stress of the triblock copolymers as a function of the PBLA content.

reduced crystallinity should give increased elasticity to the film, presumably enabling the transfer of the necking portion without breaking.

Conclusions

Symmetrical ABA triblock copolymers with a polypeptide as the A segment and PEO as the B segment with an extremely narrow molecular distribution were synthesized. The copolymers formed the translucent cast film with an excellent flexibility and strength, which were not shown in individual homopolymers. The copolymers were highly crystallized, adopting the conformation of an α-helix−7_2 helix−α-helix. These two helixes had very close pitches. The copolymer further formed a hierarchical structure; SAXD and AFM studies confirmed that the copolymer chains aggregated into a long-range structure to form a ripplelike construct, which arranged with a spacing of 150−300 Å to form a leaflike larger domain with around several nanometers in size. Spherulites were also formed over the film. This hierarchical structure may work as a framework supporting the film to impart the elasticity and strength. Elastomeric behavior was also associated with a decrease in the PEO crystallinity secondary to the influence of adjacent PBLA segments. If the copolymer was heated to over 333 K, crystals in the PEO segments melted, but the PBLA crystals remained to sustain the shape of the film, which never melted down. Successive cooling and standing at 303 K for several minutes recrystallized the spherulites, whose crystallinity was reduced. Thermal treatment induced a conformational change from an α-helix to a β-sheet, presumably in the interfacial portion between the PBLA with PEO. The formation of a β-sheet where the multiple interchain hydrogen bonds were formed imparted increased strength, and the reduced crystallinity gave increased elasticity to the film. Thus, the desired flexibility and strength of triblock copolymer films can be achieved by controlling the composition of the segments and by thermal treatment, possibly leading to the development of custom-made films in the biomedical field.

References and Notes

(1) Katchalski-Katzir, E. *Acta Biochim. Pol.* **1996**, *43*, 217.
(2) Martin, E. C.; May, P. D.; McMahon, W. *J. Biomed. Mater. Res.* **1971**, *5*, 53.
(3) Anderson, J. M.; Hiltner, A.; Schodt, K.; Woods, R. *J. Biomed. Mater. Res. Symp.* **1972**, *3*, 25.
(4) Walton, A. G. In *Biomedical Polymers*; Goldberg, E. P., Nakajima, A., Eds.; Academic Press: New York, 1980; p 53.
(5) McKeehan W. L.; Ham, R. G. *J. Cell Biol.* **1976**, *71*, 727.
(6) *Handbook of Water-Soluble Gums and Resins*; McGraw-Hill: New York, 1980; Chapter 18.
(7) *Encyclopedia of Polymer Science and Technology*; Wiley: New York, 1967; Vol. 6, pp 103−145.
(8) Bailey F. E.; Koleske, J. V. *Poly(ethylene oxide)*; Academic Press: New York, 1976; Vol. 6, pp 103−145.
(9) Makenus, J. D. *J. Am. Oil Chem. Soc.* **1956**, *33*, 571.
(10) McClelland C. P.; Batemen, R. L. *Chem. Eng. News* **1945**, *23*, 247.
(11) Shaffer, C. B.; Critchfield, F. H. *J. Am. Pharm. Assoc.* **1947**, *36*, 152.
(12) Kataoka, K.; Kwon, G. S.; Yokoyama, M.; Okano, T.; Sakurai, Y. *J. Controlled Release* **1993**, *24*, 119.
(13) Kwon, G. S.; Naito, M.; Kataoka, K.; Yokoyama, N.; Sakurai, Y.; Okano, T. *Collids Surf. B* **1994**, *2*, 429.
(14) Kugo, K.; Uno, T.; Yamano, H.; Nishino, J.; Hideo, M. *Kobunshi Ronbunshu* **1985**, *42*, 731.
(15) Cho, C. S.; Kim, S. W.; Sung, Y. K.; Kim, K. Y. *Macromol. Chem.* **1988**, *189*, 1505.
(16) Cho, C. S.; Kim S. W.; Komoto, T. *Macromol. Chem.* **1990**, *191*, 981.
(17) Floudas, G.; Papadopoulos, P.; Klok, H.-A.; Vandermeulen, G. W. M.; Rodrigues-Hernandez, J. *Macromolecules* **2003**, *36*, 3673.
(18) Fuller, W. D.; Verlander, M. S.; Goodman, M. *Biopolymers* **1976**, *15*, 869.
(19) Tadokoro, H.; Chatani, Y.; Kobayashi, M.; Yoshimura, T.; Murahashi, S.; Yamada, K. *Rep. Prog. Polym. Phys. Jpn.* **1963**, *6*, 303.
(20) Tadokoro, H.; Chatani, Y.; Yoshimura, T.; Tahara, S.; Murahashi, S. *Makromol. Chem.* **1964**, *74*, 109.
(21) Cho, C. S.; Jo, B. W.; Kwon, J. W.; Komoto, T. *Macromol. Chem. Phys.* **1994**, *195*, 2195.
(22) Hashimoto, M.; Arakawa, S. *Bull. Chem. Soc.* **1967**, *40*, 1698.
(23) Miyazacwa, T.; Blout, E. R. *J. Am. Chem. Soc.* **1961**, *83*, 712.
(24) Kubelka, J.; Keiderling, T. A. *J. Am. Chem. Soc.* **2001**, *123*, 612.
(25) Chu, H. L.; Lin, S. Y. *Biophys. Chem.* **2001**, *89*, 173.

MA035472N